Supporting Information

Thermally stable fishnet-like 1T-MoS_2/CNTs heterostructures with improved electrode performance

Zhendong Lei, Xue Yu, Yong Zhang*, Jing Zhan*

Z. D. Lei,
NUS Graduate School for Integrative Sciences and Engineering, National University of Singapore, Singapore 117456
*Xue Yu, Dr. J. Zhan**
School of Environmental and Chemical Engineering, Shanghai University, 99 Shangda Road, Shanghai, P. R. China, 200444
Z. D. Lei, Dr. J. Zhan, Prof. Yong Zhang
Department of Biomedical Engineering, Faculty of Engineering, National University of Singapore, Singapore 117583
E-mail: "Yong Zhang" biezy@nus.edu.sg; "Jing Zhan" biezhj@nus.edu.sg

Density Functional Theory Calculations.

The calculations were performed in the framework of DFT with the CASTEP program in Materials Studio by Accelrys Inc.[1] The Perdew–Burke–Ernzerhof (PBE) functional within the generalized gradient approximation (GGA) was used to evaluate the nonlocal exchange correlation energy.[2] An ultrasoft pseudopotential was used for interactions between electrons and ions.[3] A cutoff energy of 421 eV and 3*3*1 k-point grid generated with the Monk-horst– Pack scheme were used. The Grimme method were used for DFT-D correction. A vacuum of 10 Å was inserted between neighboring cells along the c-axis to minimize interactions between cells. The atomic structures were optimized using the BFGS algorithm.[4] The convergence criteria were set to: (1) an energy tolerance of $1.0e^{-5}$ eV per atom; (2) a force tolerance of 0.03 eV $Å^{-1}$; (3) a max displacement tolerance of 0.001 Å; (4) a self-consistent field tolerance of $1.0e^{-5}$ eV per atom. The transition state (TS) searches were performed at the same theoretical level with the complete linear synchronous transit/quadratic synchronous transit (LST/QST) method.[5 6] 3×3 MoS_2 and MoS_2-Graphene with ether structures were adopted for TS searches calculation and the total energy was divided by 9 to obtain the activation energy per MoS_2 unit cell.

Calculations method of specific capacity.

The specific capacity of 3D@1T-MoS_2 is calculated by removing the contribution of CNT-CFC matrix. Specifically, we calculate the specific capacity of 3D@1T-MoS_2 by using

$$SC_M = (AC_M\text{-}AC_C)/A_M$$

Where SC_M is the specific capacity of 3D@1T-MoS_2, AC_M and AC_C are the average area capacity of 3D@1T-MoS_2 and CNT-CFC, respectively. A_M is the mass loading of MoS_2 on 3D@1T-MoS_2. For example, the mass loading of MoS_2 on 3D@1T-MoS_2 is 1.00 mg cm^{-2}, the average area capacity of 3D@1T-MoS_2 is 3.942 mAh cm^{-2} at 0.1 mA cm^{-2}, and the average area capacity of CNT-CFC is 2.947 mAh cm^{-2} at 0.1 mA cm^{-2}(Fig. 4c). So, the average specific capacity of 3D@1T-MoS_2 at 0.1 mA cm^{-2} for LIBs is calculated as 995 mAh g^{-1}. The specific capacity of 3D@1T-MoS_2-700 is calculated in the same way (1.1 mg cm^{-2}).

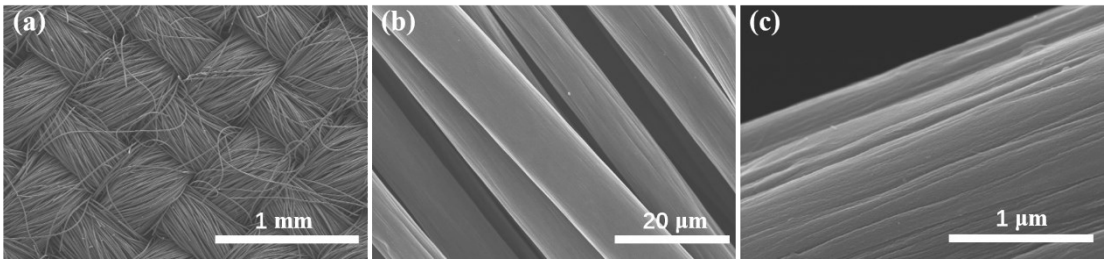

Fig. S1 SEM images of annealed CFC with different magnification (a), (b) and (c).

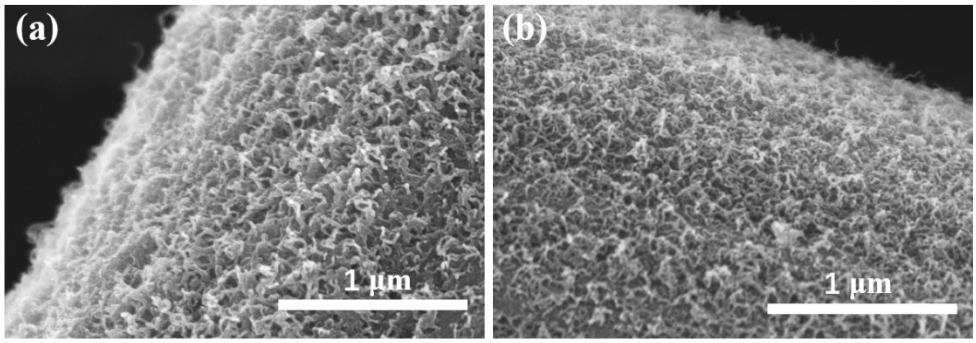

Fig. S2 SEM images of CNT-CFC (a) before and (b) after calcined at 700 ℃ in an Ar atmosphere.

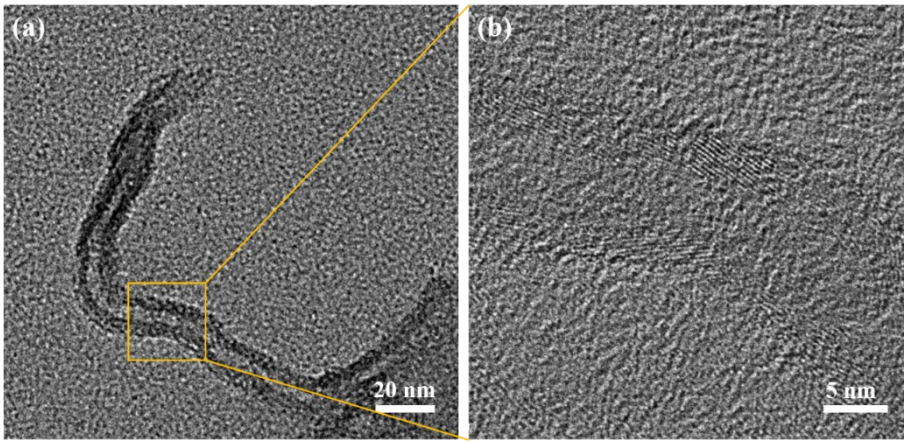

Fig. S3 TEM and HR-TEM images of CNT-CFC.

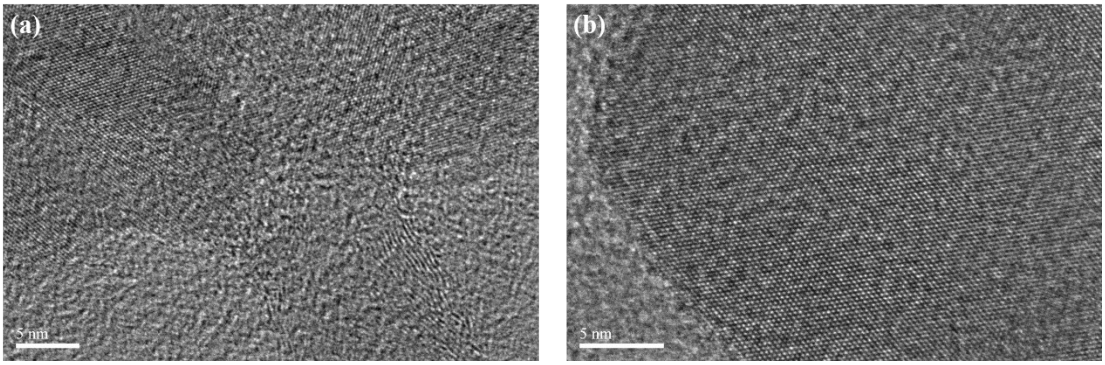

Fig. S4 HR-TEM images of 3D@1T-MoS_2-700.

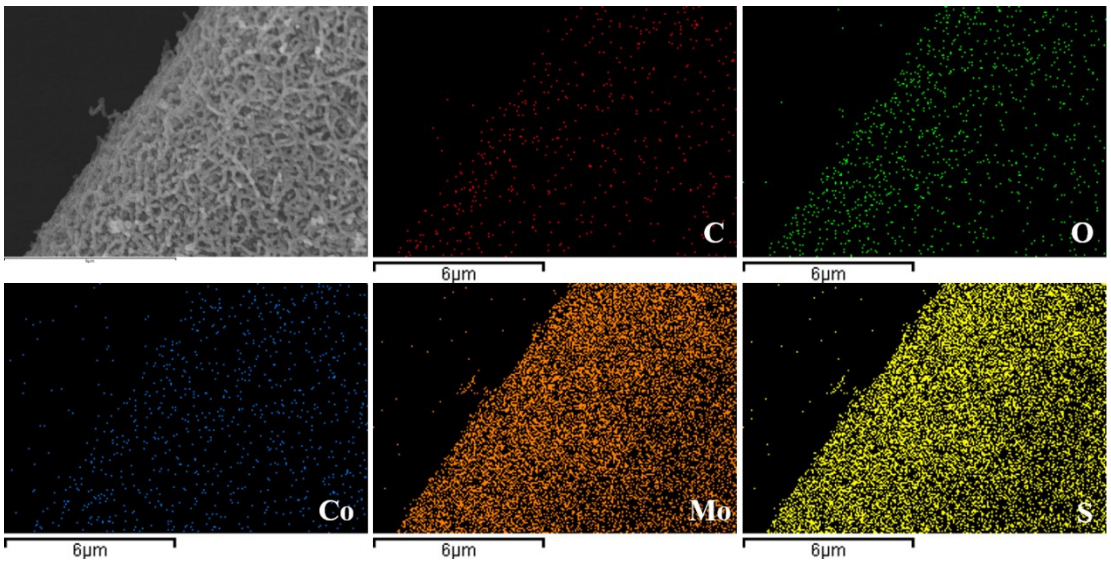

Fig. S5 SEM image of 3D@1T-MoS_2 and corresponding elemental mapping images of C (red), O (green), Co (blue), Mo (orange) and S (yellow).

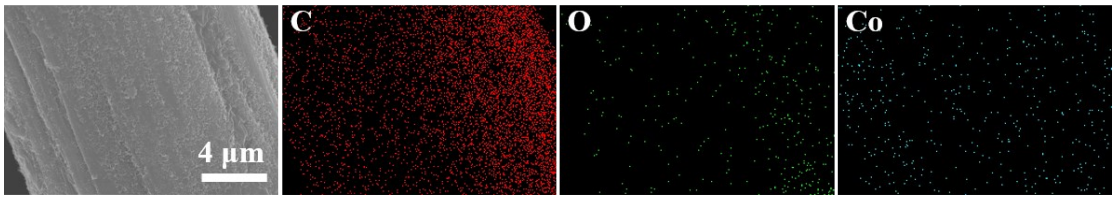

Fig. S6 SEM image of CNT-CFC and corresponding elemental mapping images of C (red), O (green) and Co (blue).

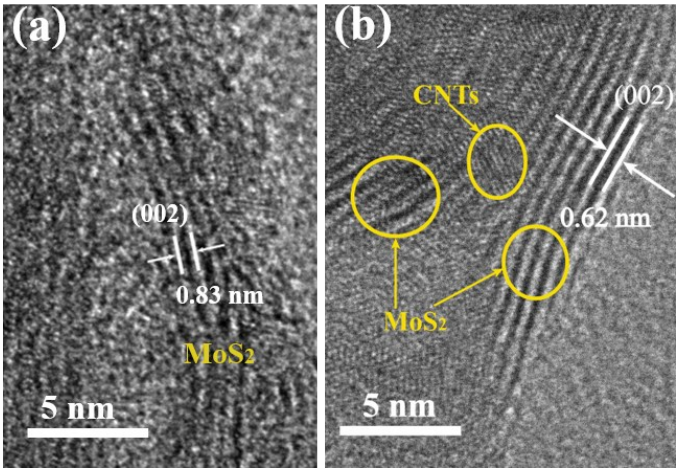

Fig. S7 HR-TEM images of (a) 3D@1T-MoS_2 and (b) 3D@1T-MoS_2-700.

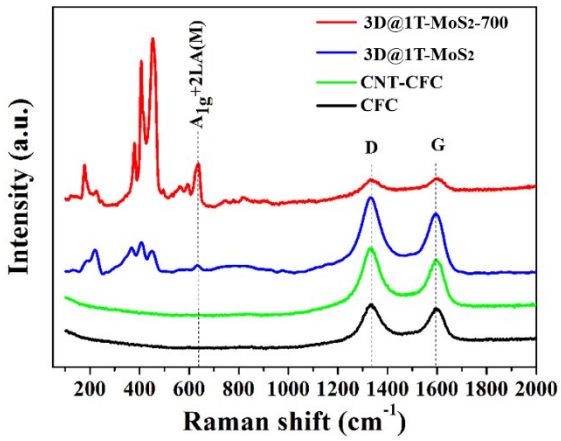

Fig. S8 Raman spectra of CFC, CNT-CFC, 3D@1T-MoS_2 and 3D@1T-MoS_2-700.

Table S1 The relative fraction of 1T components of MoS_2 nanosheets with and without CNT as a composite, before and after 700 ℃ annealing in Ar atmosphere for 2 h, estimated by the deconvolution of Mo and S XPS peaks.

materials	all%		S%		Mo%	
	1T	2H	1T	2H	1T	2H
MoS_2-CFC	51.01	48.99	53.21	46.79	48.68	51.32
MoS_2-CFC-700	0.00	100.00	0.00	100.00	0.00	100.00
3D@1T-MoS_2	38.20	61.80	51.27	48.73	26.87	73.13
3D@1T-MoS_2-600	76.51	23.49	68.35	31.65	84.67	15.33
3D@1T-MoS_2-700	62.12	37.88	56.25	43.75	67.76	32.24

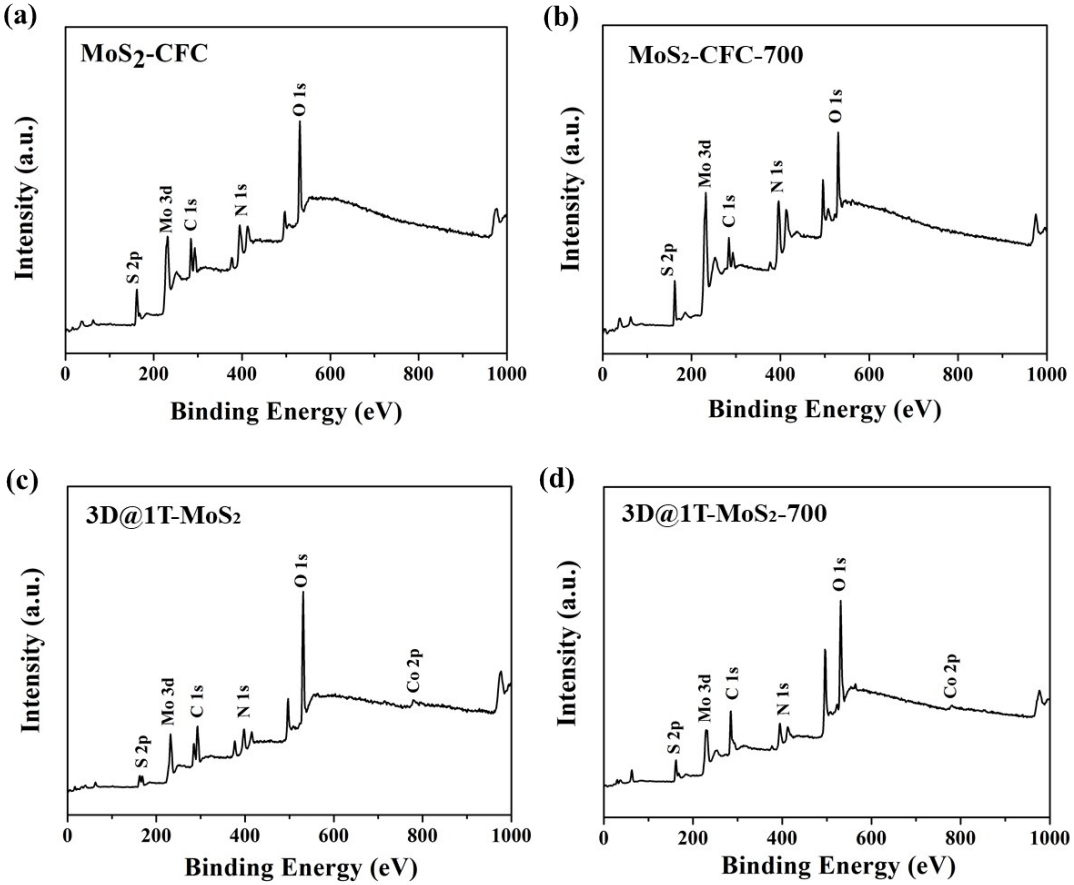

Fig. S9 Survey XPS spectrum of (a) MoS_2-CFC, (b) MoS_2-CFC-700, (c) 3D@1T-MoS_2 and (d) 3D@1T-MoS_2-700.

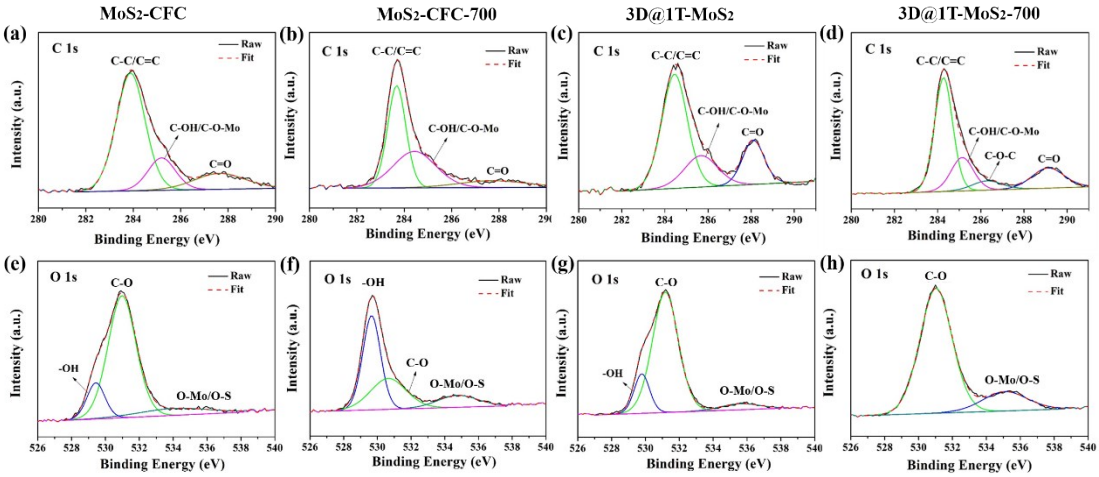

Fig. S10 High-resolution XPS C 1s and O 1s spectra of the four selected samples. Each band was deconvoluted following the literature.

Rate constant based on the Arrhenius-type equation

$$k = Ae^{-E_a/RT} \longrightarrow \frac{k_{MoS_2}}{k_{MoS_2/CNT}} = \frac{Ae^{-0.712/0.025}}{Ae^{-0.900/0.025}} \approx 1.8 \times 10^3$$

$E_a = \Delta E * 1.6e^{-19} * 6.02e^{23}\ \mathrm{J} \cdot mol^{-1}$
$R = 8.314\ J \cdot mol^{-1}K^{-1}$
$T = 298.15\ K$

Fig. S11 As based on the Arrhenius-type equation with the calculated activation energy difference, CNTs binding on MoS_2 slows down the phase transition about 1845 times.

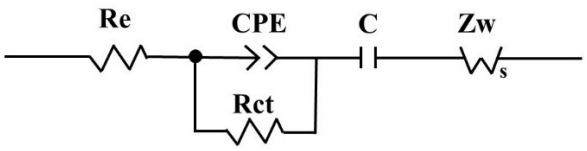

Fig. S12 Equivalent circuit model to fit the Nyquist plots. Re is the resistance of electrolyte diffusion (the intercept of the semicircle at the imaginary axis); Rct is the charge-transfer resistance within the composites (the diameter of the semicircle); Zw is the Warburg-type resistance caused by ion diffusion in the electrode (the oblique inclined line in the low-frequency region).

Table S2 Equivalent circuit parameters of CFC, CNT-CFC, MoS_2-CFC, MoS_2-CFC-700, 3D@1T-MoS_2 and 3D@1T-MoS_2-700.

Electrode	***Re(Ω)***	***Rct(Ω)***
CFC	5.002	299.8
CNT-CFC	6.783	23.98
MoS_2-CFC	10.14	8.032
MoS_2-CFC-700	5.242	24.00
3D@1T-MoS_2	6.944	37.21
3D@1T-MoS_2-700	2.261	15.52

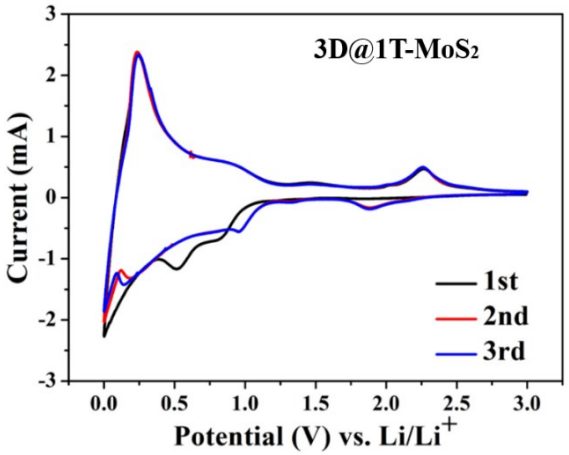

Fig. S13 CV curves of 3D@1T-MoS_2 electrodes at a scan rate of 0.1 mV s^{-1} between 0.01 and 3.0 V.

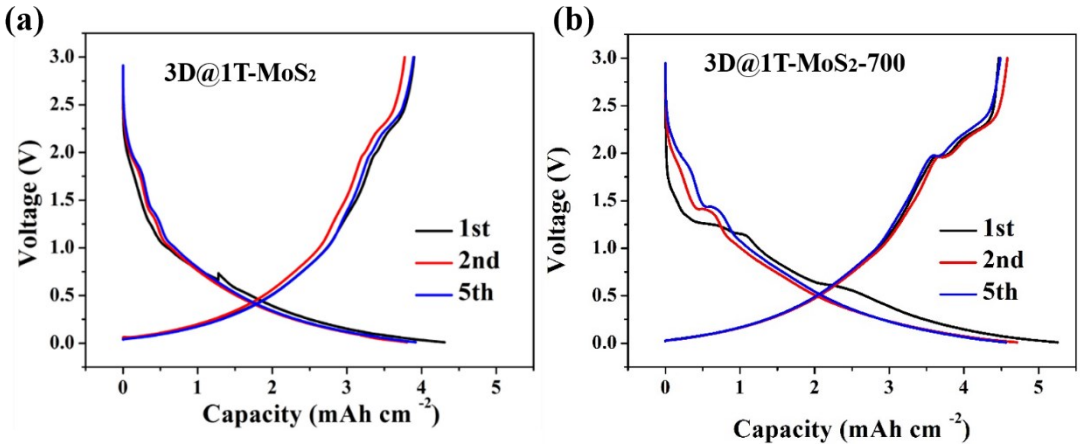

Fig. S14 Discharge and charge voltage profiles of (a) 3D@1T-MoS_2 and (b) 3D@1T-MoS_2-700 electrode at a current density of 0.1 mA cm^{-2} for different cycles.

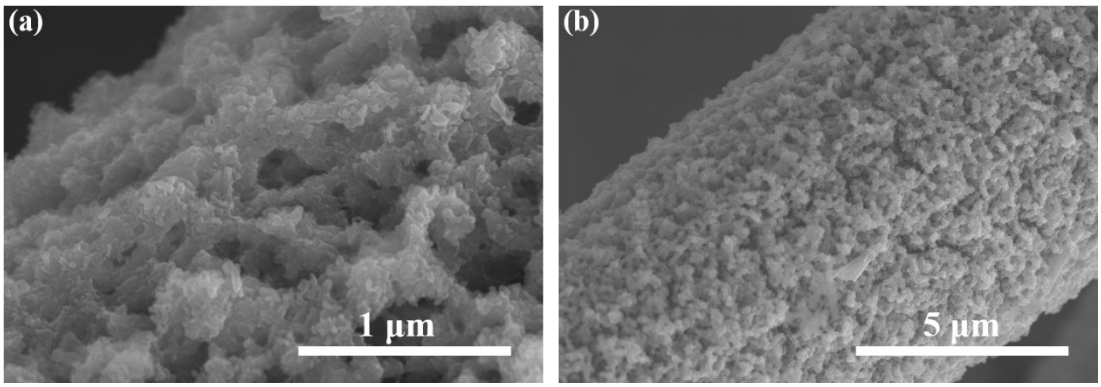

Fig. S15 (a,b) SEM images of 3D@1T-MoS_2-700 electrodes discharged to 0.01 V at current densities of 0.1 mA cm^{-2} in the first cycle.

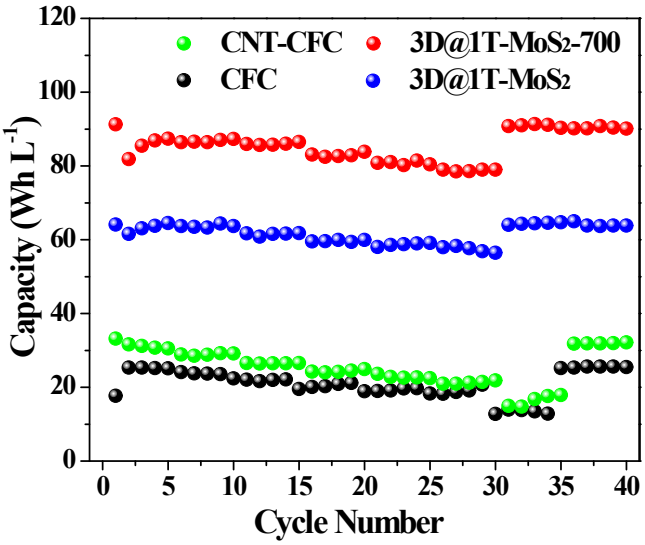

Fig. S16 The volume energy density of the CFC, CNT-CFC, 3D@1T-MoS_2, and 3D@1T-MoS_2-700 electrodes at different current densities (The area of the electrode material is 1.13094 cm^2. The thickness of the electrode material is 0.337±0.010 mm.).

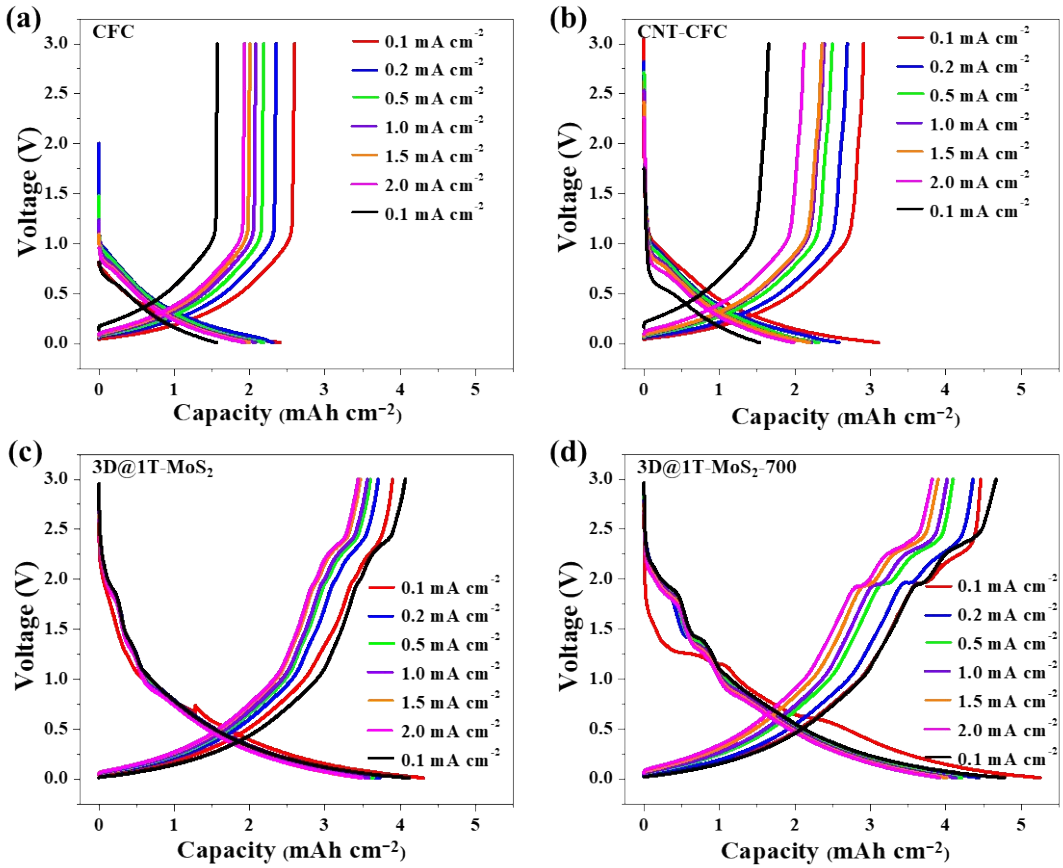

Fig. S17 The galvanostatic discharge and charge voltage profiles of (a) CFC, (b) CNT-CFC, (c) 3D@1T-MoS_2 and (d) 3D@1T-MoS_2-700 electrode at different current densities.

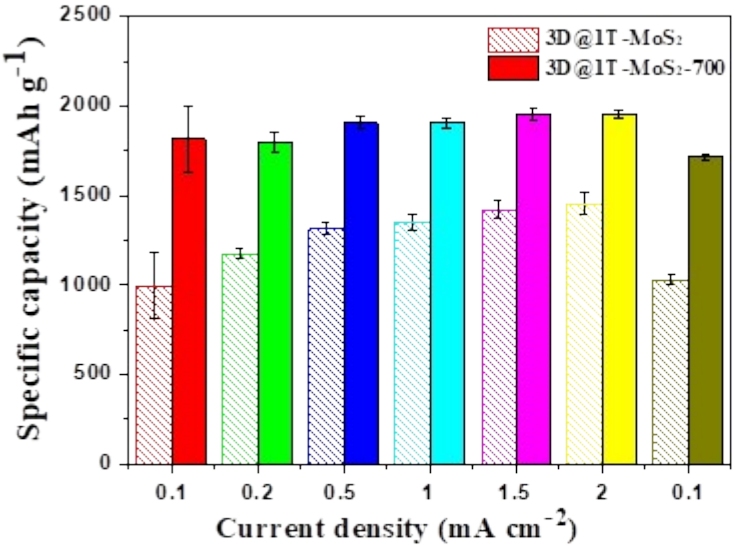

Fig. S18 The calculated specific capacity of 3D@1T-MoS_2 and 3D@1T-MoS_2-700 for LIBs.

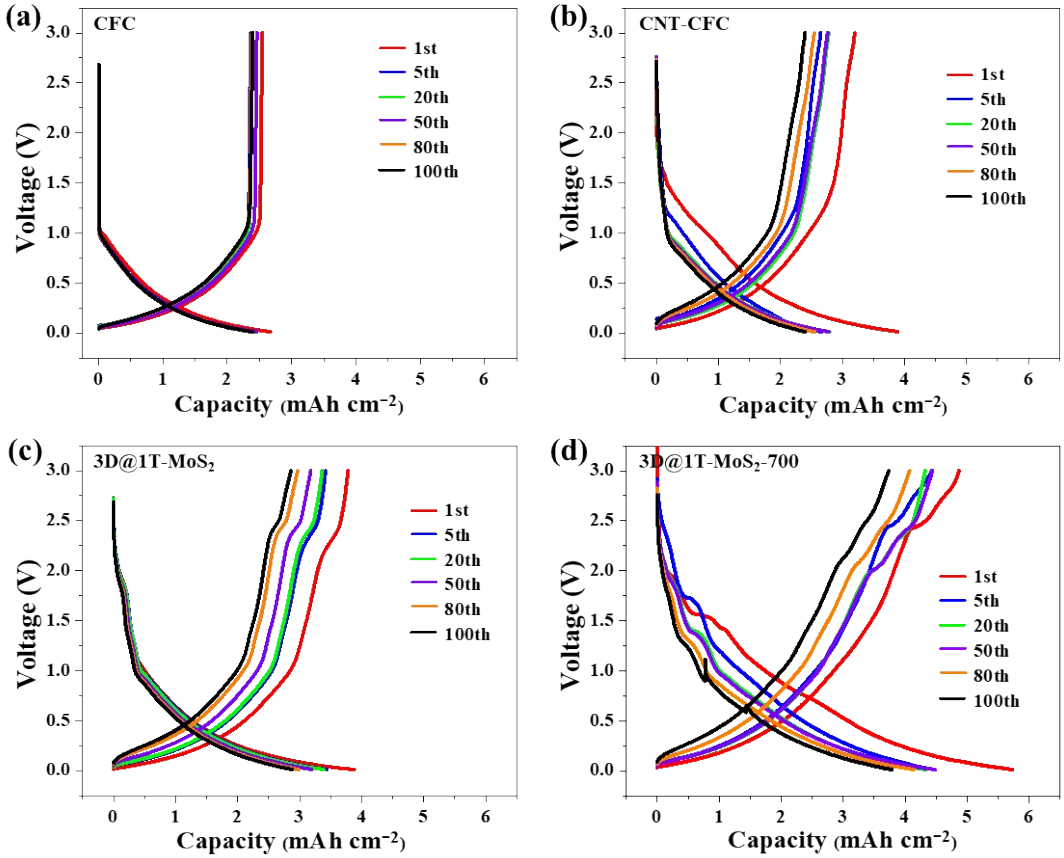

Fig. S19 The galvanostatic discharge and charge voltage profiles of (a) CFC, (b) CNT-CFC, (c) 3D@1T-MoS_2 and (d) 3D@1T-MoS_2-700 electrode at a current density of 0.5 mA cm^{-2} for different cycles.

Reference:

[1]. J. Clark Stewart, D. Segall Matthew, J. Pickard Chris, J. Hasnip Phil, I. J. Probert Matt, K. Refson and C. Payne Mike, Z. Kristallogr., 2005, 220, 567.

[2]. J. P. Perdew, K. Burke and M. Ernzerhof, Phys. Rev. Lett., 1996, 77, 3865-3868.

[3]. D. Vanderbilt, Phys. Rev. B: Condens. Matter Mater. Phys., 1990, 41, 7892-7895.

[4]. B. G. Pfrommer, M. Coˆte ´, S. G. Louie and M. L. Cohen, J. Comput. Phys., 1997, 131, 233-240.

[5]. N. Govind, M. Petersen, G. Fitzgerald, D. King-Smith and J. Andzelm, Comput. Mater. Sci., 2003, 28, 250-258.

[6]. T. A. Halgren and W. N. Lipscomb, Chem. Phys. Lett., 1977, 49, 225-232.